

Reinforcement Learning-based Self-adaptive Differential Evolution through Automated Landscape Feature Learning

Hongshu Guo
guohongshu369@gmail.com
South China University of Technology
Guangzhou, Guangdong, China

Sijie Ma
masijie9@gmail.com
South China University of Technology
Guangzhou, Guangdong, China

Zechuan Huang
hohqhzc825@gmail.com
South China University of Technology
Guangzhou, Guangdong, China

Yuzhi Hu
goodd0z1y@gmail.com
South China University of Technology
Guangzhou, Guangdong, China

Zeyuan Ma
scut.crazy nicolas@gmail.com
South China University of Technology
Guangzhou, Guangdong, China

Xinglin Zhang
csxlzhang@scut.edu.cn
South China University of Technology
Guangzhou, Guangdong, China

Yue-Jiao Gong*
gongyuejiao@gmail.com
South China University of Technology
Guangzhou, Guangdong, China

Abstract

Recently, Meta-Black-Box-Optimization (MetaBBO) methods significantly enhance the performance of traditional black-box optimizers through meta-learning flexible and generalizable meta-level policies that excel in dynamic algorithm configuration (DAC) tasks within the low-level optimization, reducing the expertise required to adapt optimizers for novel optimization tasks. Though promising, existing MetaBBO methods heavily rely on human-crafted feature extraction approach to secure learning effectiveness. To address this issue, this paper introduces a novel MetaBBO method that supports automated feature learning during the meta-learning process, termed as RLDE-AFL, which integrates a learnable feature extraction module into a reinforcement learning-based DE method to learn both the feature encoding and meta-level policy. Specifically, we design an attention-based neural network with mantissa-exponent based embedding to transform the solution populations and corresponding objective values during the low-level optimization into expressive landscape features. We further incorporate a comprehensive algorithm configuration space including diverse DE operators into a reinforcement learning-aided DAC paradigm to unleash the behavior diversity and performance of the proposed RLDE-AFL. Extensive benchmark results show that co-training the proposed feature learning module and DAC policy contributes to the superior optimization performance of RLDE-AFL to several advanced DE methods and recent MetaBBO baselines over both synthetic and realistic BBO scenarios. The source codes of RLDE-AFL are available at <https://github.com/GMC-DRL/RLDE-AFL>.

CCS Concepts

• **Computing methodologies** → **Bio-inspired approaches; Reinforcement learning**; *Markov decision processes*.

Keywords

Automatic configuration, differential evolution, reinforcement learning, meta-black-box optimization

*Corresponding author.

1 Introduction

In the last few decades, Evolutionary Computation (EC) methods such as Genetic Algorithm (GA) [13], Particle Swarm Optimization (PSO) [21] and Differential Evolution (DE) [52] have become more and more eye-catching in solving Black-Box Optimization (BBO) problems lacking accessible formulations or derivative information in both academia and industry [35]. However, according to the “No-Free-Lunch” (NFL) theorem [62], no single algorithm or algorithm configuration (AC) can dominate on all problems. Therefore, to enhance the optimization performance on diverse problems, researchers have manually designed various adaptive operator selection and parameter control methods, which achieve superior performance on BBO benchmarks [12, 33, 38]. However, the design of the operator and parameter adaptive mechanisms requires substantial experience and deep expertise in optimization problems and algorithms. One may need to adjust the configurations iteratively according to the problem characteristic and optimization feedback, consuming significant time and computational resources.

To relieve the human effort burden, recent researchers introduce Meta-Black-Box Optimization (MetaBBO) which leverages a meta-level policy to replace the human-crafted algorithm designs in Algorithm Selection [10], Algorithm Configuration [28, 32, 48, 53], Solution Manipulation [23–25, 64] and Algorithm Generation [7, 34, 75]. MetaBBO methods typically involve a bi-level architecture. In the meta level, given the optimization state, a neural network based policy determines an appropriate algorithm design for the low-level algorithm at each optimization generation. The resulting changes in objective values after algorithm optimization are returned to the meta-level policy as meta performance signal, which is then used to refine the meta policy [35, 68]. Given the meta policy π_θ parameterized by θ with the algorithm A on a set of problem instances \mathcal{I} , the objective for algorithm configuration is formulated as:

$$\mathbb{J}(\theta) = \arg \max_{\theta \in \Theta} \mathbb{E}_{f \in \mathcal{I}} \left[\sum_{t=1}^T \text{Perf}(A, \omega_t, f) \right] \quad (1)$$

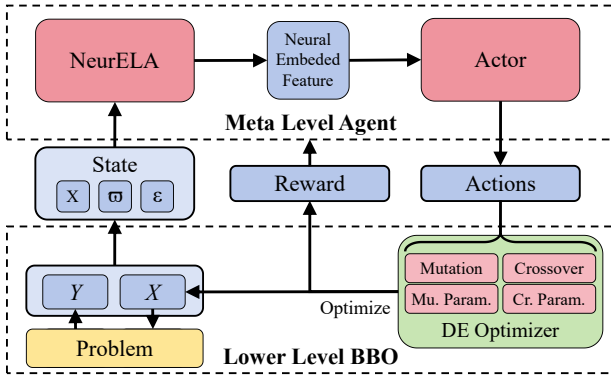


Figure 1: The overview of the bi-level structure in RLDE-AFL.

where T is the optimization horizon, $Perf(\cdot)$ is a performance metric function, $\omega_t = \pi_\theta(s_t)$ is the algorithm design outputted by the policy and s_t is the optimization state at generation t . For algorithm configuration, ω may correspond to operator selection, parameter values, or both. To maximize the expected performance on the problem distribution, machine learning methods such as Reinforcement Learning (RL) are widely adopted for policy training.

Though promising, these works still retain significant potential to further reduce the expertise burden and enhance the performance. The first limitation is the expertise dependent optimization state design, which requires substantial domain to develop informing and representative features for comprehensive configurations. Besides, while traditional BBO community have developed diverse operator variants, existing MetaBBO methods typically adopt only a small subset of these operators, leading to a limited strategy diversity. Moreover, the configuration spaces in existing MetaBBO methods are restricted, most works focus on exclusively operator selection [48, 54] or parameter control [32, 53], failing to fully unleash the behavior diversity of the meta policies.

To address these issues, we propose RLDE-AFL. Firstly, for the expertise-dependent state representation, we employ NeurELA [31], as shown in the top left of Figure 1, a self-attention neural network based optimization information extractor to automatically analyze the problem landscape from the population and evaluation values, eliminating the need for manual feature design. The two-stage self-attention between the dimensions and individuals achieves generalizable and comprehensive state extraction. By integrating the mantissa-exponent based evaluation value representation, we further enhance the generalization ability of RLDE-AFL.

Then, to further enhance the performance of RLDE-AFL, we integrate 14 DE mutation operators and 3 DE crossover operators with diverse optimization behaviours to form the candidate operator pool (illustrated in the bottom right of Figure 1). This diversity enables the agent to adaptively deploy distinct optimization strategies tailored to different problem instances. By incorporating parameter control, RL agent gains full control over the DE framework through optimization states derived from the automatic feature extractor, thereby unleashing the behavior diversity of RL agent to achieve superior performance.

Finally, we conduct extensive experiments to demonstrate the effectiveness of RLDE-AFL on MetaBox [33] benchmark problems. The comparisons with advanced traditional DE algorithms and RL-based DE methods confirm the superior performance of RLDE-AFL. The zero-shot performance on different dimensional problems, expensive problems and out-of-distribution realistic problems shows the robust generalization capabilities of RLDE-AFL, outperforming existing advanced traditional and learning based methods.

The rest of this paper is organized as follows: Section 2 reviews the related works on existing traditional adaptive DE. Section 3 introduces the preliminary concepts on RL and NeurELA. In Section 4, we present our technical details, including the Markov Decision Process (MDP) definition, network design and training process. The experimental results are presented in Section 5, followed by a conclusion in Section 6.

2 Related Works

2.1 Traditional AC for DE

For DE algorithms, the algorithm configurations usually focus on selecting mutation and crossover operators and controlling the parameters of these operators. In vanilla DE [52], the used operator and parameters are static across optimization horizon and problem instances. However, since the landscapes and characteristics of BBO problems can vary, static configurations may not be optimal.

In the last few decades, DE community has proposed diverse mutation and crossover operators with diverse exploratory and exploitative behaviours. Combining these operators using adaptive operator selection mechanisms is a promising approach for superior performance. SaDE [43] assigns each individual mutation operators selected from the two candidate operators following the probabilities calculated from operators' historical performance. CoDE [60] integrates 3 mutation-crossover combinations and selects the best one among the 3 individuals generated by the three combinations as the offspring. LADE [26] assigns different mutation operators for different sub-populations to enhance the population diversity.

To further enhance the behavior diversity and improve algorithm performance, jDE [4] randomly generates scale factor F for mutation and crossover rate Cr for crossover operators, then keeps the parameters that successfully improved individuals. One of the advanced variant of jDE, JDE21 [5] introduces multi-population mechanism and divides the population into exploratory one and exploitative one with different parameter and operator configurations. However, random searching parameter configurations is not efficient. JADE [74] samples parameters from normal or Cauchy distribution with the mean updated by the Lehmer mean of the parameter values that successfully improve the individuals in last generation. Based on JADE, SHADE [57] uses two memories to record the Lehmer mean of F and Cr respectively in each generation, which enhances the exploration. Such successful history based parameter adaptive mechanism is widely adopted in advanced DE variants such as MadDE [2], NL-SHADE-LBC [49] and L-SRTDE [51].

Although these mechanisms bring significant performance [22, 38, 42], one must equip with enough expert knowledge on the algorithm and optimization problem to design suitable operator selection rules and parameter adaptive mechanisms, which leads to heavy human-effort burden.

2.2 MetaBBO-RL based AC for DE

To relieve the burden, researchers turn to machine learning for answers. One of the most commonly adopted solution is to use Reinforcement Learning (RL) agents to learn the knowledge about optimization and dynamically determine the operator selection and parameter control according to the optimization states. For operator selection, value-based RL methods such as Tabular Q-Learning [61] and Deep Q-Learning [37] are widely adopted to handle the discrete action spaces. Tabular Q-Learning maintains a table mapping each discrete state to an optimal action [9, 11, 14, 17, 27, 45, 66, 73]. For instance, RLDMD [67] selects mutation-crossover operator combinations for each sub-population according to the population diversity levels. However, the coarse-grained discrete state spaces may lead to information loss and degrade the performance. Therefore, neural networks are introduced to process continuous states and predict the expected accumulated reward of each candidate action, which turns to Deep Q-Network (DQN) [39, 48, 54, 73]. DE-DDQN [48] designs a 99-dimensional continuous state including the optimization status and operator performance history. A Multilayer Perceptron (MLP) based Double DQN [58] agent is employed to determine the mutation operator for each individual. Though promising, the complex state design significantly slows down the time efficiency. DE-DQN [54] uses Fitness Landscape Analysis (FLA) [63] to extract 4 optimization features from random walk sampling, which are then feed into a DQN agent for operator selection. Besides, neural networks can also be used to predict the probabilities of action selection [16, 28, 29, 72]. RLEMMO [28] uses the agent trained by Proximal Policy Optimization (PPO) [46] to select DE mutation operators for solving multi-modal problems. Furthermore, some methods consider the whole DE algorithms as switchable components. RL-DAS [10] selects algorithms periodically from three advanced candidate DE algorithms according to the optimization status and algorithm histories.

For parameter control, some methods discretize the continuous action space and use Q-Learning to select the parameter values [15, 18, 70]. RLMODE [70] uses the feasible and domination relationship of individuals as the states to control increasing or decreasing the values of scale factors and crossover rates for solving constrained multi-objective problems. More RL-based parameter control methods for DE use neural networks to predict the distribution of the target parameters [30, 32, 40, 53, 65, 71]. LDE [53] leverages Long Short-Term Memory (LSTM) network to sequentially determine the values of scale factors and crossover rates for each individual according to the population fitness histograms. GLEET [32] further proposes a Transformer-based architecture [59] to balance the exploration-exploitation in DE and PSO by using parameter control. There are also works that control both operator and parameters [55]. RL-HPSDE [55] employs Q-table to select the combinations of operator and parameter sampling methods.

Although these RL based adaptive methods achieve remarkable optimization performance, they still face three limitations. Firstly, the design of state features still require expertise on optimization problems and algorithms so that features can be properly selected to reflect the optimization status. Besides, some features need extra function evaluations for random sampling which occupy the

resource for optimization. Secondly, the collected candidate operators in the operator pools of existing methods are limited, only a small number of operators are considered, which limits the strategy diversity and generalization. Finally, most of these methods focus on selecting operators only or controlling parameters only, the learning and generalization ability of RL agents are not fully developed. To address these limitations, we hence in this paper propose RLDE-AFL, which introduces automatic learning based state representation and integrates diverse operators fully controlled by the RL agent for superior performance.

3 Preliminary

3.1 Markov Decision Process

A MDP could be denoted as $\mathcal{M} := \langle \mathcal{S}, \mathcal{A}, \mathcal{T}, R \rangle$. Given a state $s_t \in \mathcal{S}$ at time step t , the policy π accordingly determines an action $a_t \in \mathcal{A}$ which interacts with the environment. The next state s_{t+1} is produced by the changed environment through the environment dynamic $\mathcal{T}(s_{t+1}|s_t, a_t)$. A reward function $R: \mathcal{S} \times \mathcal{A} \rightarrow \mathbb{R}$ acts as a performance metric measuring the performance of the actions. Those transitions between states and actions achieve a trajectory $\tau := (s_0, a_0, s_1, \dots, s_T)$. The target of MDP is to find an optimal policy π^* that maximizes the accumulated rewards in trajectories:

$$\pi^* = \arg \max_{\pi \in \Pi} \sum_{t=1}^T \gamma^{t-1} R(s_t, a_t) \quad (2)$$

where $\Pi: \mathcal{S} \rightarrow \mathcal{A}$ selects an action with a given state, γ is a discount factor and T is the length of trajectory.

3.2 Neural Evolutionary Landscape Analysis

To obtain the optimization status or the problem characteristic, various landscape analysis methods such as Evolutionary Landscape Analysis (ELA) have emerged. Although these approaches provide a comprehensive understanding, they require a certain level of expert knowledge and consume non-negligible computational resource. To address these issues, learning-based ELA methods are proposed to use neural networks to analyze landscapes [41, 47]. However, these methods are constrained by problem dimensions or profile problems statically, which makes them not applicable for the feature extraction in MetaBBO. Recently, Ma et al. [31] proposes Neural Exploratory Landscape Analysis (NeurELA), which employs a two-stage attention-based neural network as a feature extractor. Given a population $X \in \mathbb{R}^{N \times D}$ with N D -dimensional solutions and its corresponding evaluation values $Y \in \mathbb{R}^N$, the observations o are organized as per-dimensional tuples $\{(X_{i,j}, Y_i)\}_{i=1}^N \}_{j=1}^D$, with a shape of $D \times N \times 2$. Then o is embedded by a linear layer and advanced the two-stage attention for information sharing in cross-solution and cross-dimension levels, respectively. The cross-solution attention uses an attention block to enable same dimensions shared by different candidate solutions within the population to exchange information, while the cross-dimension attention further promotes the sharing of information across different dimensions within each candidate. In this way, NeurELA efficiently extracts comprehensive optimization state information for each individual automatically. The attention-based architectures on both dimension and solution

levels boost the scalability of NeurELA across different problem dimensions and different algorithm population sizes.

4 Methodology

4.1 MDP Formulation

At the t -th generation, given a state $s_t = \{X_t, Y_t, t\}$ including the population $X_t \in \mathbb{R}^{N \times D}$ with N D -dimensional individuals and the corresponding evaluation values $Y_t = f(X_t)$ under problem instance f , in the meta level the RLDE-AFL policy π_θ parameterized by θ extracts the optimization features of all individuals using the modified NeurELA module from s_t , then determines the operator selection and parameter control actions $a_t \sim \pi_\theta(s_t)$ for each individual. With a_t as configurations, the DE algorithm in the lower level optimize the population and produces the next state $s_{t+1} = \{X_{t+1}, Y_{t+1}, t+1\}$. The reward function R is introduced to evaluate the performance improvement $r_t = R(s_t, a_t|f)$. Considering a set of problem instances \mathcal{I} , RL agent targets at finding an optimal policy π_{θ^*} which maximizes the expected accumulated rewards over all problem instances $f \in \mathcal{I}$:

$$\theta^* = \arg \max_{\theta \in \Theta} \mathbb{E}_{f \in \mathcal{I}} \left[\sum_{t=1}^T \gamma^{t-1} R(s_t, \pi_\theta(s_t)|f) \right] \quad (3)$$

In this paper, we use the Proximal Policy Optimization (PPO) [46] to train the policy. Next we introduce the detailed MDP designs, including the state, action and reward in the following subsections.

4.1.1 State. As mentioned above, the state comprises the population solutions $X_t = \{x_{t,i}\}_{i=1}^N$ and evaluation values $Y_t \in \mathbb{R}^N$ which indicates the optimization situation, and the time stamp $t \in [1, T]$ indicating the optimization progress. Since the searching spaces of different optimization problems vary, we normalize the solution values with the upper and lower bounds of the searching space: $x'_{t,i} = \{\frac{x_{t,i,j} - lb_j}{ub_j - lb_j}\}_{j=1}^D$ where ub_j and lb_j are the upper and lower bounds of the searching space at the j -th dimension, respectively. Besides, the objective value scales across different problem instances can also vary, to ensure state values across problem instances share the same numerical level, we introduce the mantissa-exponent representation for the evaluation value terms in states. Specifically, for each evaluation value $y_{t,i} \in Y_t$, we first represent it in scientific notation $y_{t,i} = \omega \times 10^e$, $\omega \in [-1, 1]$, $e \in \mathbb{Z}$. Then we use a tuple $\{\omega_{t,i}, \epsilon_{t,i}\}$ as the mantissa-exponent representation of $y_{t,i}$ in the state, where $\epsilon = \frac{e}{\eta}$ and η is a scale factor making the scales of exponents in all problem instances similar. For the time stamp t in the state, we normalize it with the optimization horizon T so that it would share the same scale with other features: $s_{time} = \frac{t}{T}$. In summary, the state at generation t is represented as $s_t = \{ \{ \{ \frac{x_{t,i,j} - lb_j}{ub_j - lb_j} \}_{j=1}^D \}_{i=1}^N, \{ \{ \omega_{t,i}, \epsilon_{t,i} \}_{i=1}^N, s_{time} \}$, and the observation o_t for NeurELA module is changed to $\{ \{ (x_{t,i,j}, \omega_{t,i}, \epsilon_{t,i}) \}_{i=1}^N \}_{j=1}^D$.

4.1.2 Action. For operator selection we integrate 14 mutation operators and 3 crossover operators form various DE variants.

- (1) Mutation operators 1~7 are basic mutation operators in vanilla DE [52]: *rand/1*, *best/1*, *rand/2*, *best/2*, *current-to-rand/1*, *current-to-best/1* and *rand-to-best/1*, which have diverse preferences on exploration or exploitation.

- (2) Mutation operator 8~11 are the variants of the basic operators: *current-to-pbest/1*, *current-to-pbest/1 + archive*, *current-to-rand/1 + archive* and *weighted-rand-to-pbest/1*. They introduce the ‘‘pbest’’ technique which replace the best individual by randomly selected top individuals and employ the archive of the eliminated individuals to enhance the exploration.
- (3) Mutation operator 12 *ProDE-rand/1* [8] is a variant of *rand/1* which selects random individuals according to the probabilities inversely proportional to distances between individuals.
- (4) Mutation operator 13 *HARDDDE-current-to-pbest/2* [36] improves the optimization performance by introducing time stamps to the archive in *current-to-pbest/1* and sampling random individuals from the two archives containing recent individuals and former individuals respectively.
- (5) Mutation operator 14 *TopoDE-rand/1* [44] enhances the exploitation of *rand/1* by using the nearest best individual to the current individual as x_{r1} .
- (6) Crossover operator 1~2 are basic crossover operators proposed in vanilla DE [52]: *binomial* and *exponential* crossover.
- (7) Crossover operator 3 *p-binomial* crossover is a variant of *binomial* crossover which borrows the idea of ‘‘pbest’’ and replace the parent individual in the crossover with a randomly selected top individual.

In the action space for each individual we include two actions for operator selection $a^{os1} \in [1, 14]$ and $a^{os2} \in [1, 3]$. The detailed introduction of the operators are shown in Table I in Appendix A.

Besides, fine-tuning the parameters of the selected operators is also a key to superior performance. Therefore, the action space for each individual in this paper includes two parameter control actions $a^{pc1} \in [0, 1]^{M_1}$ and $a^{pc2} \in [0, 1]^{M_2}$ for the selected mutation operators and crossover operators respectively. M_1 and M_2 are the maximal numbers of parameters of all integrated mutation and crossover operators respectively. In summary, the overall action space for the population at generation t is $a_t = \{ (a_{i,t}^{os1}, a_{i,t}^{pc1}, a_{i,t}^{os2}, a_{i,t}^{pc2}) \}_{i=1}^N$.

4.1.3 Reward. We use the reward function formulated as follow:

$$r_t = \frac{y_{t-1}^* - y_t^*}{y_0^* - y^*} \quad (4)$$

where y_t^* is the found best evaluation at generation t , y_0^* is the best value in the initial population and y^* is the global optimal evaluation value of the problem instance. The accumulated rewards reflects the optimization performance, and the denominator normalizes all reward values into $[0, 1]$ to make the scales of the accumulated rewards in all problems similar, hence stabilize the training.

4.2 Network Design

4.2.1 Embedding. As shown in Figure 2, given the state s , we first reorganize the population X and evaluation values Y into the observation $o \in \mathbb{R}^{D \times N \times 3}$ as mentioned in Section 4.1.1. Then o is embedded by a linear embedder $\mathbf{h}^{(0)} = \phi(o, \mathbf{W}_e^{ob})$ where $\phi(\cdot, \mathbf{W}_e^{ob})$ denotes a MLP layer with shape 3×64 .

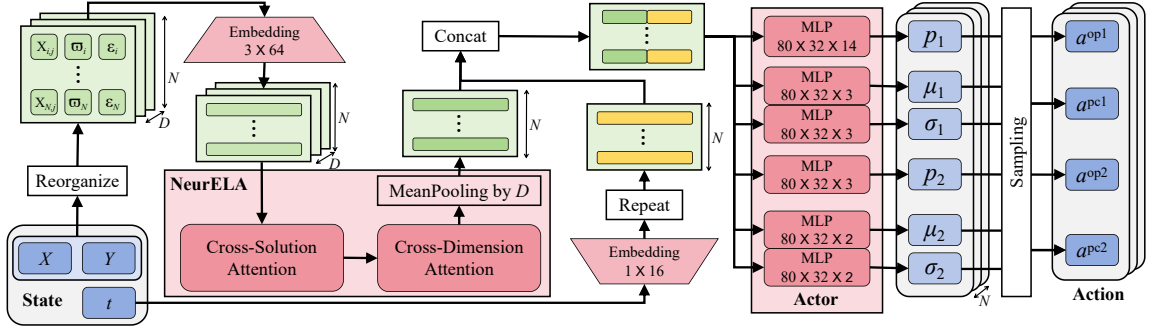


Figure 2: Illustration of the network structure.

4.2.2 *NeurELA*. The hidden representation $\mathbf{h}^{(0)} \in \mathbb{R}^{D \times N \times 64}$ is next encoded by the two-stage NeurELA module. In the cross-solution attention, information are shared between the representations of all solutions at the same dimension:

$$\begin{aligned} \hat{\mathbf{h}}^{(1)} &= \text{LN}(\text{MSA}_S(\mathbf{h}^{(0)}) + \mathbf{h}^{(0)}) \\ \mathbf{h}^{(1)} &= \text{LN}(\phi(\hat{\mathbf{h}}^{(1)}; \mathbf{W}_S^{(1)}) + \hat{\mathbf{h}}^{(1)}) \end{aligned} \quad (5)$$

where LN denotes the Layernorm [1], MSA_S is the Multi-head Self-Attention [59] in the solution dimension and $\phi(\cdot; \mathbf{W}_S^{(1)})$ is a MLP layer with the shape of 64×64 . In the cross-dimension attention, the encoded results $\mathbf{h}^{(1)}$ from the cross-solution attention is transposed to $N \times D \times 64$ and augmented with cosine/sine positional encodings to maintain the dimensional order within a solution.

$$\mathbf{h}'^{(1)} = (\mathbf{h}^{(1)})^T + \mathbf{W}_{pos} \quad (6)$$

where \mathbf{W}_{pos} is the positional encoding weights. Subsequently, we conduct the feature extraction to discover the inner connections between the dimensions:

$$\begin{aligned} \hat{\mathbf{h}}^{(2)} &= \text{LN}(\text{MSA}_D(\mathbf{h}'^{(1)}) + \mathbf{h}'^{(1)}) \\ \mathbf{h}^{(2)} &= \text{LN}(\phi(\hat{\mathbf{h}}^{(2)}; \mathbf{W}_D^{(2)}) + \hat{\mathbf{h}}^{(2)}) \end{aligned} \quad (7)$$

where MSA_D is the self-attention module between the dimensions and $\phi(\cdot; \mathbf{W}_D^{(2)})$ is also a MLP layer with the shape of 64×64 . The encoded individual representations $\mathbf{e}_{xy} \in \mathbb{R}^{N \times 64}$ is obtained by meanpooling $\mathbf{h}^{(2)} \in \mathbb{R}^{N \times D \times 64}$ in the second dimension.

4.2.3 *Time stamp feature*. To take time stamp information into consideration when determining the actions, we embed s_{time} into a 16-dimensional representation $\mathbf{e}_{time} = \phi(s_{time}; \mathbf{W}_T)$ where $\phi(\cdot; \mathbf{W}_T)$ is also a MLP layer with the shape of 1×16 . Then repeat it for N times to match the shape of \mathbf{e}_{xy} : $\mathbf{e}_{time} = \{\mathbf{e}_{time}\}_{i=1}^N$. The decision vector $\mathbf{d}\mathbf{v} \in \mathbb{R}^{N \times (64+16)}$ is obtained as the concatenation of \mathbf{e}_{xy} and \mathbf{e}_{time} : $\mathbf{d}\mathbf{v} = \text{Concat}(\mathbf{e}_{xy}, \mathbf{e}_{time})$.

4.2.4 *Actor*. Finally, the probabilities of selecting mutation operators p_1 , probabilities of selecting crossover operators p_2 , distribution of the parameters for mutation $\mathcal{N}(\mu_1, \sigma_1)$ and distribution of the parameters for crossover $\mathcal{N}(\mu_2, \sigma_2)$ for each individual are obtained through the MLP layers in the Actor separately as illustrated in the right of Figure 2. For instance, to select the mutation operator of the i -th individual, its decision vector is mapped

Algorithm 1: Pseudo Code of the training of RLDE-AFL

Input: Policy π_θ , Critic V_ψ , Training instance Set $\mathcal{I}_{\text{train}}$
Output: Trained Policy π_θ , Critic V_ψ

```

for epoch = 1 to Epoch do
    for  $f \in \mathcal{I}_{\text{train}}$  do
        Initialize population  $X_1$  and evaluation values  $Y_1 = f(X_1)$ ;
        for  $t = 1$  to  $T$  do
            Obtain state  $s_t$  using  $X_t, Y_t$  and  $t$ ;
            Determine actions  $a_t = \pi_\theta(s_t)$ ;
            Optimize  $X_t$  using DE with configurations  $a_t$  and
            obtain  $X_{t+1}, Y_{t+1}$ ;
            Calculate reward  $r_t$  following Eq. (4);
            Collect the transition  $\langle s_t, a_t, s_{t+1}, r_t \rangle$ ;
            if  $\text{mod}(t, n) == 0$  then
                for  $k = 1$  to  $\kappa$  do
                    Update  $\pi_\theta$  and  $V_\psi$  by PPO method;
                end
            end
        end
    end

```

to the 14-dimensional probability vector corresponding to the 14 candidate mutation operators: $p_{1,i} = \text{Softmax}(\phi(\mathbf{d}\mathbf{v}_i; \mathbf{W}_M))$ by the MLP $\phi(\cdot; \mathbf{W}_M)$ with shape $80 \times 32 \times 14$, and the index of the selected operator is sampled from $\text{Categorical}(p_{1,i})$. The parameters of the selected mutation operator is sampled from the normal distribution $a_i^{pc1} \sim \mathcal{N}(\phi(\mathbf{d}\mathbf{v}_i; \mathbf{W}_{M\mu}), \text{Diag}(\phi(\mathbf{d}\mathbf{v}_i; \mathbf{W}_{M\sigma})))$ where $\phi(\cdot; \mathbf{W}_{M\mu})$ and $\phi(\cdot; \mathbf{W}_{M\sigma})$ are two MLP layers with the same shape of $80 \times 32 \times 3$. It is worth noting that for parameter control, to uniformly control all operators which have diverse numbers of parameters, we pre-defined the maximum parameter numbers for mutation and crossover operators (in this paper, they are 3 and 2 respectively). The MLPs in Actor output 3 or 2 parameter for all operators. If the operator needs less parameters, the first few values would be used and the rest are ignored.

4.2.5 *Critic*. For the critic V_ψ parameterized by ψ , we calculate the value of an individual as $V_\psi(s_i) = \phi(\mathbf{d}\mathbf{v}_i; \mathbf{W}_C)$ using a MLP with the shape of $80 \times 16 \times 8 \times 1$ and ReLU activation functions. The value of the population is the averaged value per individual $V_\psi(s) = \frac{1}{N} \sum_{i=1}^N V_\psi(s_i)$.

Table 1: The comparison results of the baselines on 10D testing problems.

	Traditional DE Variants						RL-based DE Variants						
	DE	MadDE	JDE21	NL-SHADE-LBC	AMCDE	Random	DE-DDQN	DE-DQN	LDE	RL-HPSDE	GLEET	RL-DAS	RLDE-AFL
F1	4.584e1 ±6.640e0 ⁺	2.614e1 ±5.528e0 ⁺	3.051e1 ±1.415e1 ⁺	1.653e1 ± 4.289e0 ≈	3.161e1 ±1.417e1 ⁺	3.032e1 ±7.238e0 ⁺	4.004e1 ±7.818e0 ⁺	3.118e2 ±6.292e1 ⁺	3.471e1 ±4.974e0 ⁺	7.457e1 ±1.040e1 ⁺	2.815e1 ±5.718e0 ⁺	3.400e1 ±6.207e0 ⁺	1.811e1 ±7.333e0 ⁺
F2	9.325e-1 ±3.203e-1 ⁺	1.170e-2 ±6.815e-3 ⁺	4.893e-2 ±2.101e-1 ⁺	1.846e-1 ±1.371e-1 ⁺	4.423e0 ±7.042e0 ⁺	1.521e-2 ±4.300e-2 ⁺	4.669e-1 ±3.250e0 ⁺	4.678e4 ±2.687e4 ⁺	1.290e-1 ±1.329e-1 ⁺	1.204e1 ±4.692e0 ⁺	4.251e-1 ±1.662e-1 ⁺	3.743e-2 ±1.841e-2 ⁺	2.525e-7 ± 2.205e-7
F3	1.575e0 ±3.954e-1 ⁺	4.395e-1 ±2.559e-1 [≈]	7.377e-1 ±4.520e-1 ⁺	2.993e-2 ±6.775e-2 ⁻	2.218e0 ±8.504e-1 ⁺	2.571e-1 ±1.616e-1 [≈]	5.655e-3 ± 3.999e-2	1.807e2 ±6.459e1 ⁺	3.401e-1 ±4.349e-1 [≈]	2.792e0 ±1.591e0 ⁺	2.359e-2 ±2.600e-2 [≈]	6.781e-1 ±3.084e-1 ⁺	3.719e-1 ±3.830e-1
F4	8.196e0 ±4.098e0 ⁺	5.044e0 ±4.435e-1 ⁺	3.359e0 ±2.082e0 ⁺	4.557e0 ±7.521e-1 ⁺	1.365e1 ±2.285e1 [≈]	6.570e0 ±8.534e-1 ⁺	8.239e-1 ± 1.877e0	1.499e4 ±7.657e3 ⁺	5.407e0 ±1.995e0 ⁺	5.312e1 ±3.281e1 ⁺	6.248e0 ±9.377e-1 ⁺	5.417e0 ±9.221e-1 ⁺	1.514e0 ±1.093e0
F5	7.506e0 ±2.479e-1 ⁺	3.254e0 ±6.338e-1 ⁺	6.780e0 ±2.738e0 ⁺	6.944e0 ±6.599e-1 ⁺	8.237e0 ±7.712e0 ⁺	7.372e0 ±4.360e-1 ⁺	2.431e0 ±2.492e0 [≈]	1.258e4 ±5.998e3 ⁺	7.088e0 ±9.246e-1 ⁺	4.327e1 ±2.368e1 ⁺	6.478e0 ±7.257e-1 ⁺	4.363e0 ±8.598e-1 ⁺	2.407e0 ± 1.182e0
F6	1.380e4 ±8.229e3 ⁺	8.980e2 ±5.369e2 ⁺	6.242e2 ±6.666e2 ⁺	9.828e1 ±8.054e1 ⁺	2.839e3 ±1.131e3 ⁺	2.588e3 ±1.023e3 ⁺	4.560e1 ±2.147e2 ⁺	5.294e5 ±3.317e5 ⁺	2.206e2 ±2.227e2 [≈]	2.621e3 ±2.232e3 ⁺	1.723e1 ± 1.643e1	1.387e3 ±8.063e2 ⁺	1.530e2 ±1.444e2 ⁺
F7	1.344e2 ±2.775e1 ⁺	2.949e1 ±1.125e1 ⁺	8.144e0 ±8.448e0 ⁺	8.617e0 ±4.953e0 ⁺	1.543e2 ±3.598e1 ⁺	2.977e1 ±9.567e0 ⁺	7.803e0 ±6.936e0 ⁺	8.445e0 ±1.446e3 ⁺	2.593e1 ±5.847e0 ⁺	2.593e1 ±5.232e1 ⁺	3.484e1 ± 1.147e1	3.414e0 ±9.974e0 ⁺	3.414e0 ±2.532e0
F8	1.369e3 ±1.196e3 ⁺	8.770e1 ±6.079e1 ⁺	8.144e0 ±9.372e0 ⁺	2.285e0 ±2.077e0 ⁺	7.474e3 ±4.546e3 ⁺	5.916e6 ±1.772e6 ⁺	1.211e4 ±6.156e4 ⁺	2.924e7 ±9.112e6 ⁺	3.627e0 ±2.712e0 ⁺	1.992e5 ±1.578e5 ⁺	2.942e1 ±1.950e1 ⁺	7.466e1 ±6.990e1 ⁺	1.240e0 ± 1.575e0
F9	1.380e1 ±3.017e0 ⁺	2.358e0 ±8.985e-1 ⁺	5.347e0 ±7.360e0 [≈]	1.023e-1 ±1.827e-1 ⁻	1.561e1 ±4.849e0 ⁺	4.783e0 ±1.832e0 ⁺	1.042e-6 ± 4.091e-7	9.133e2 ±1.664e2 ⁺	5.508e-1 ±9.579e-1 ⁻	7.408e1 ±2.781e1 ⁺	1.254e0 ±5.199e-1 [≈]	3.124e0 ±1.405e0 [≈]	2.908e0 ±3.724e0
F10	3.599e-3 ±8.465e-4 ⁺	8.888e-4 ±4.605e-4 ⁺	4.771e-4 ±3.167e-4 ⁺	7.050e-5 ±5.500e-5 [≈]	3.025e-3 ±1.414e-2 ⁻	4.252e-4 ±2.705e-4 ⁺	2.637e-8 ± 1.276e-7	1.193e1 ±4.089e0 ⁺	2.611e-4 ±1.704e-4 ⁺	2.080e-1 ±1.373e-1 ⁺	1.996e-4 ±1.118e-4 ⁺	1.570e-3 ±4.325e-4 ⁺	6.642e-5 ±3.046e-5
F11	1.510e0 ±3.539e-1 ⁺	1.435e0 ±4.560e-1 ⁺	8.793e-1 ±7.375e-1 ⁺	1.257e-1 ±7.574e-2 ⁺	4.087e0 ±1.314e0 ⁺	2.361e-2 ±3.254e-2 ⁻	3.786e-3 ± 1.742e-2	4.839e0 ±6.330e0 ⁺	3.505e-1 ±2.517e-1 ⁺	4.839e0 ±1.536e0 ⁺	2.035e1 ±2.08e-1 ⁺	2.035e1 ±4.582e-1 ⁺	7.239e-2 ±9.005e-2
F12	2.946e0 ±4.763e-1 ⁺	1.138e0 ±4.309e-1 ⁺	2.501e0 ±4.347e-1 ⁺	2.200e0 ±4.661e-1 ⁺	1.795e0 ±1.308e0 ⁺	2.279e0 ±4.367e-1 ⁺	2.279e0 ±5.311e-1 ⁺	1.209e1 ±2.158e0 ⁺	2.069e0 ±3.717e-1 ⁺	2.069e0 ±6.716e-1 ⁺	4.256e0 ±4.858e-1 ⁺	9.524e-1 ±2.673e-1 ⁺	6.821e-1 ± 6.788e-1
F13	1.610e0 ±1.802e-1 ⁺	8.774e-1 ±1.687e-1 ⁺	4.500e-1 ±2.202e-1 ⁻	2.477e-1 ± 1.674e-1	1.514e0 ±2.063e-1 ⁻	4.497e-1 ±2.208e-1 ⁻	1.640e0 ±3.319e-1 ⁺	7.034e3 ±2.884e3 ⁺	1.491e0 ±3.024e-1 ⁺	2.386e0 ±1.696e-1 ⁺	1.091e0 ±2.146e-1 ⁺	1.059e0 ±2.536e-1 ⁺	6.569e-1 ±2.343e-1
F14	3.638e0 1.000e0 ⁺	5.860e-1 ±2.263e-1 [≈]	1.118e0 ±7.399e-1 [≈]	6.666e-1 ±1.251e-1 [≈]	1.705e0 ±8.843e-1 [≈]	2.631e0 ±2.232e0 ⁺	8.157e-1 ±3.756e-1 [≈]	5.254e1 ±1.298e1 ⁺	6.093e-1 ±1.936e-1 [≈]	2.964e0 ±1.844e0 ⁺	6.805e-1 ±2.331e-1 [≈]	5.895e-1 ±2.205e-1 [≈]	2.439e0 ±2.302e0
F15	1.837e0 ±3.562e-1 ⁺	1.337e0 ±3.141e-1 ⁺	1.414e0 ±2.419e-1 ⁺	1.360e0 ±2.802e-1 ⁺	1.930e0 ±2.836e-1 ⁺	1.523e0 ±2.916e-1 ⁺	1.313e0 ±1.999e-1 ⁺	3.477e0 ±9.457e-1 ⁺	1.374e0 ±2.926e-1 ⁺	1.782e0 ±3.684e-1 ⁺	1.252e0 ±2.708e-1 ⁺	1.393e0 ±1.212e-1 ⁺	1.105e0 ± 4.564e-1
F16	3.992e1 ±5.603e0 ⁺	4.178e1 ±6.003e0 ⁺	3.841e1 ±8.614e0 ⁺	3.581e1 ±6.988e0 ⁺	5.055e1 ±7.247e0 ⁺	3.706e1 ±7.623e0 ⁺	4.177e1 ±5.589e0 ⁺	1.686e2 ±2.163e1 ⁺	4.138e1 ±3.673e0 ⁺	6.822e1 ±7.224e0 ⁺	4.157e1 ±6.349e0 ⁺	4.411e1 ±6.492e0 ⁺	2.217e1 ± 6.183e0
+ / - / ≈	16 / 0 / 0	13 / 0 / 3	13 / 1 / 2	9 / 4 / 3	13 / 1 / 2	13 / 2 / 1	8 / 6 / 2	16 / 0 / 0	12 / 1 / 3	16 / 0 / 0	11 / 2 / 3	15 / 0 / 1	N/A

4.3 Training

In this paper we use the n -step PPO [46] to train the policy in RLDE-AFL. As illustrated in Algorithm 1, given a training problem instance set $\mathcal{I}_{\text{train}}$, for each epoch and each problem instance $f \in \mathcal{I}_{\text{train}}$, the DE algorithm first initializes a $N \times D$ population and evaluate it using f . For each generation t , the state s_t is collected as mentioned in Section 4.1.1. The policy π_θ determines the action a_t including the selected mutation and crossover operators and their corresponding parameters according to the state. With these configurations the DE algorithm optimize the population for one generation and obtain the next state s_{t+1} and reward r_t . The transition $\langle s_t, a_t, s_{t+1}, r_t \rangle$ is appended into a memory. For each n generations, the actor π_θ and critic V_ψ are updated for κ steps using PPO manner.

5 Experiment

In this section, we discuss the following research questions: **RQ1**: How does the proposed RLDE-AFL perform on synthetic problem instances? **RQ2**: Can RLDE-AFL zero-shot to synthetic problems with expensive evaluation costs or different dimensions, as well as realistic problems? **RQ3**: How does the design of feature extractor affect RLDE-AFL’s performance? Below, we first introduce the experimental settings and then address RQ1~RQ3 respectively.

5.1 Experimental Setup

5.1.1 Training setup. The following experiments are based on the MetaBox Benchmark [33] which provides the synthetic CoCo-BBOB benchmark [12], the noisy-synthetic benchmark [12] and the Protein-Docking benchmark [19]. In this paper we use 8 of the 24 problem instances with dimensions of 10 in the synthetic

benchmark as training problem set $\mathcal{I}_{\text{train}}$ and the rest 16 problem instances as testing set (F1~F16). The detailed problem formulation and train-test split are provided in Appendix B. We train the policy for 100 epochs with a learning rate of $1e-3$ and Adam optimizer. The PPO process is conducted $\kappa = 3$ steps for every $n = 10$ generation with discount factor $\gamma = 0.99$. For the DE optimization, the population size N is set to 100, the maximum function evaluations is 20,000 thus the optimization horizon $T = 200$. The searching space of all problem instances are $[-5, 5]^D$. All baselines in all experiments are run for 51 times. All experiments are run on Intel(R) Xeon(R) E5-2678 CPU and NVIDIA GeForce 1080Ti GPU with 32G RAM.

5.1.2 Baselines. MetaBox integrates a large number of classic and advanced DE algorithms. In this paper we adopt vanilla DE [52], advanced DE variants MadDE [3], JDE21 [6], NL-SHADE-LBC [50] and AMCDE [69] as traditional DE baselines. Besides, we include the random action RLDE-AFL without RL agent (denoted as “Random”) to validate the effectiveness of RL training. For RL-based baselines, we adopt operator selection methods DE-DDQN [48], DE-DQN [54], parameter control methods LDE [53], GLEET [32], method that conducts both operator selection and parameter control RL-HPSDE [56] and algorithm selection method RL-DAS [10]. The configurations of these baselines follow the setting in their original papers. RL-based baselines are trained on the same $\mathcal{I}_{\text{train}}$ with the same number of learning steps as RLDE-AFL for fair comparisons.

5.2 Comparison on 10D Testing Set (RQ1)

In this section we compare the optimization performance of our proposed RLDE-AFL with the baselines to answer RQ1. We train RLDE-AFL and RL-based baselines on the 8 problem instance $\mathcal{I}_{\text{train}}$

Table 2: The comparison results of the baselines on 20D testing problems. RL-DAS fails to generalize to 20D problems and is marked as “/” due to its problem dimension-dependent feature design.

	Traditional DE Variants						RL-based DE Variants						
	DE	MadDE	JDE21	NL-SHADE-LBC	AMCDE	Random	DE-DDQN	DE-DQN	LDE	RL-HPSDE	GLEET	RL-DAS	RLDE-AFL
F1	1.882e2 ±1.563e1 ⁺	1.935e2 ±1.528e1 ⁺	1.470e2 ±4.598e1 ⁺	1.040e2 ±1.598e1 ⁺	4.708e2 ±1.105e2 ⁺	3.195e2 ±7.503e1 ⁺	1.494e2 ±2.528e1 ⁺	1.201e3 ±2.781e2 ⁺	1.367e2 ±1.689e1 ⁺	2.948e2 ±4.318e1 ⁺	1.385e2 ±1.444e1 ⁺	/	5.309e1 ±1.559e1
F2	6.017e1 ±9.446e0 ⁺	4.013e1 ±4.998e0 ⁺	1.320e1 ±1.426e1 ⁺	1.188e1 ±4.803e0 ⁺	4.051e2 ±1.661e2 ⁺	1.012e2 ±6.252e1 ⁺	1.077e1 ±1.382e1 ⁺	1.265e5 ±5.919e4 ⁺	6.539e0 ±3.717e0 ⁺	1.929e2 ±3.054e1 ⁺	1.816e1 ±4.907e0 ⁺	/	1.033e-1 ±1.319e-1
F3	3.755e1 ±7.877e0 ⁺	1.598e1 ±3.362e0 ⁺	1.137e1 ±7.579e0 ⁺	2.798e0 ±1.026e0 ⁻	7.321e1 ±1.616e1 ⁺	5.703e1 ±2.681e1 ⁺	7.478e0 ±7.017e0 [≈]	5.881e2 ±1.345e2 ⁺	7.896e0 ±2.971e0 ⁺	4.479e1 ±2.070e1 ⁺	3.839e0 ±1.451e0 ⁻	/	6.225e0 ±3.929e0
F4	6.885e1 ±1.836e1 ⁺	1.039e2 ±1.951e1 ⁺	4.256e1 ±3.212e1 ⁺	1.689e1 ±6.453e-1 ⁺	2.059e3 ±2.578e3 ⁺	1.599e2 ±8.383e1 ⁺	6.275e1 ±4.567e1 ⁺	1.335e5 ±3.857e4 ⁺	5.084e1 ±3.004e1 ⁺	1.069e3 ±6.218e2 ⁺	2.701e1 ±1.516e1 ⁺	/	1.745e1 ±1.548e1
F5	3.206e1 ±5.580e0 ⁺	3.356e1 ±1.030e1 ⁺	3.299e1 ±2.766e1 ⁺	1.832e1 ±7.480e-1 ⁺	8.553e3 ±6.270e3 ⁺	1.161e2 ±1.796e1 ⁺	1.966e1 ±5.498e0 ⁺	7.805e4 ±2.019e4 ⁺	1.854e1 ±6.756e0 ⁺	6.568e2 ±4.247e2 ⁺	1.875e1 ±1.097e0 ⁺	/	1.423e1 ±6.982e0
F6	2.281e5 ±5.702e4 ⁺	2.856e4 ±6.367e3 ⁺	1.070e4 ±7.056e3 ⁺	4.260e3 ±1.412e3 ⁺	2.006e5 ±5.102e4 ⁺	3.678e4 ±2.996e4 ⁺	7.251e2 ±3.789e3 ⁺	1.937e6 ±6.158e5 ⁺	4.689e3 ±1.767e3 ⁺	1.050e5 ±5.803e4 ⁺	2.992e3 ±1.406e3 ⁺	/	4.700e3 ±1.913e3
F7	2.863e2 ±3.913e1 ⁺	7.694e1 ±1.265e1 ⁺	6.420e1 ±1.998e1 ⁺	3.377e1 ±9.034e0 ⁻	3.440e2 ±4.995e1 ⁺	9.865e1 ±3.796e1 ⁺	3.162e1 ±9.994e0 ⁻	1.682e8 ±2.411e3 ⁺	4.300e1 ±9.238e0 ⁻	1.268e2 ±4.995e1 ⁺	1.054e1 ±5.289e0 ⁻	/	5.096e1 ±1.108e1
F8	7.019e4 ±3.034e4 ⁺	1.437e5 ±5.586e4 ⁺	1.186e3 ±8.341e3 [≈]	1.550e2 ±3.021e2 ⁺	9.262e6 ±2.599e6 ⁺	1.302e6 ±4.642e6 ⁺	5.609e6 ±1.118e7 ⁺	1.682e8 ±4.063e7 ⁺	7.870e0 ±1.292e1 ⁺	5.778e6 ±2.675e6 ⁺	6.007e3 ±2.486e3 ⁺	/	4.590e0 ±6.529e0
F9	1.014e2 ±1.307e1 ⁺	1.156e2 ±1.709e1 ⁺	3.106e1 ±2.600e1 [≈]	2.385e1 ±5.755e0 [≈]	5.438e2 ±6.236e1 ⁺	2.517e2 ±1.352e2 ⁺	1.292e2 ±6.969e1 ⁺	1.861e3 ±1.863e2 ⁺	6.266e1 ±1.779e1 ⁺	3.772e2 ±1.057e2 ⁺	2.697e1 ±7.85e0 [≈]	/	2.427e1 ±2.134e1
F10	1.422e-1 ±3.063e-2 ⁺	1.182e-1 ±3.807e-2 ⁺	6.561e-3 ±5.119e-3 ⁺	2.250e-3 ±9.769e-4 ⁺	4.823e0 ±9.922e-1 ⁺	4.444e-1 ±3.564e-1 ⁺	3.585e-1 ±4.326e-1 ⁺	3.394e1 ±7.914e0 ⁺	5.238e-3 ±2.398e-3 ⁺	3.211e0 ±1.500e0 ⁺	1.634e-2 ±6.760e-3 ⁺	/	9.519e-4 ±5.232e-4
F11	9.217e0 ±1.420e0 ⁺	8.668e0 ±1.432e0 ⁺	4.928e0 ±2.658e0 ⁺	9.403e-1 ±4.131e-1 ⁺	1.778e1 ±2.345e0 ⁺	1.717e1 ±4.165e0 ⁺	1.823e0 ±1.160e0 ⁺	4.629e1 ±4.713e0 ⁺	1.896e0 ±7.897e-1 ⁺	3.284e0 ±2.574e0 ⁺	1.558e1 ±1.015e0 ⁺	/	4.828e-1 ±4.071e-1
F12	5.729e0 ±5.177e-1 ⁺	3.804e0 ±4.603e-1 [≈]	4.888e0 ±6.351e-1 ⁺	4.801e0 ±4.913e-1 ⁺	7.365e0 ±6.496e-1 ⁺	2.504e-1 ±9.903e-5 ⁻	4.826e0 ±3.498e-1 ⁺	2.052e1 ±2.492e0 ⁺	4.339e0 ±3.452e-1 ⁺	6.671e0 ±7.936e-1 ⁺	4.461e0 ±6.467e-1 ⁺	/	3.301e0 ±1.362e0
F13	2.667e0 ±1.361e-1 ⁺	2.348e0 ±1.274e-1 ⁺	9.133e-1 ±1.933e-1 ⁻	1.435e0 ±1.930e-1 ⁺	1.836e1 ±3.228e1 ⁺	6.684e0 ±3.077e1 ⁺	2.670e0 ±1.876e-1 ⁺	3.529e4 ±1.060e4 ⁺	2.296e0 ±1.037e-1 ⁺	1.224e1 ±4.386e1 ⁺	2.098e0 ±1.561e-1 ⁺	/	1.109e0 ±1.796e-1
F14	1.712e1 ±8.110e0 ⁺	8.914e0 ±3.003e-1 ⁺	9.162e0 ±4.979e0 ⁺	8.113e0 ±2.164e0 ⁺	4.562e1 ±1.108e1 ⁺	1.304e1 ±8.494e0 ⁺	1.229e1 ±7.759e0 ⁺	7.855e1 ±2.890e0 ⁺	7.721e0 ±2.609e0 ⁺	1.490e1 ±8.964e0 ⁺	6.398e0 ±3.650e0 ⁺	/	1.043e1 ±6.426e0
F15	3.171e0 ±5.202e-1 ⁺	2.478e0 ±3.177e-1 ⁺	2.343e0 ±3.829e-1 [≈]	2.415e0 ±3.670e-1 [≈]	3.630e0 ±5.854e-1 ⁺	2.52e0 ±8.491e-1 [≈]	2.288e0 ±3.562e-1 [≈]	4.156e0 ±7.387e-1 ⁺	2.430e0 ±3.896e-1 ⁺	2.709e0 ±3.974e-1 ⁺	2.112e0 ±4.176e-1 [≈]	/	2.23e0 ±4.864e-1
F16	1.650e2 ±1.069e1 ⁺	1.677e2 ±8.599e0 ⁺	1.219e2 ±1.844e1 [≈]	1.244e2 ±1.091e1 ⁺	2.262e2 ±2.286e1 ⁺	1.923e2 ±3.426e1 ⁺	1.336e2 ±1.358e1 ⁺	4.757e2 ±4.756e1 ⁺	1.305e2 ±8.811e0 ⁺	2.006e2 ±1.658e1 ⁺	1.278e2 ±1.276e1 ⁺	/	1.127e2 ±1.966e1
+ / - / ≈	16 / 0 / 0	15 / 0 / 1	11 / 1 / 4	11 / 2 / 3	16 / 0 / 0	14 / 1 / 1	12 / 2 / 2	16 / 0 / 0	14 / 1 / 1	16 / 0 / 0	11 / 3 / 2	/	N/A

and test them on F1~F16. The mean and standard deviation of the 51 runs for all baselines are presented in Table 1. The ‘+’, ‘-’ and ‘≈’ indicate the statistical test results that the performance of RLDE-AFL is better, worse and no significant difference with competing methods respectively according to the Wilcoxon rank-sum test at the 0.05 significance level. The results show that:

- (1) Our RLDE-AFL outperforms all traditional and RL-based baselines, achieving the state-of-the-art performance, which validates the effectiveness of the proposed method.
- (2) RLDE-AFL significantly surpasses the random action baseline which reveals the advantage of RL-based configuration policy and validates the effectiveness of the RL training. Besides, the random action baselines outperforms DE which reveals that integrating diverse operators would enhance the robustness of algorithm and lead to certain performance even using random operator selection and parameters.
- (3) Compared to traditional baselines, the RL based configuration policy in RLDE-AFL shows superior performance than human-crafted adaptive mechanisms, indicating that RL agents could not only relieve the expertise dependence in adaptive mechanism designs, but also present promising optimization performance.
- (4) Compared to RL-based baselines using human-crafted features, the superior performance of RLDE-AFL validates the effectiveness of the NeurELA based feature extraction. Besides, instead of exclusively selecting operators or controlling parameters, including both operator selection and parameter control for individuals in action space could

minimize the expertise dependence, unleash the behavior diversity, and hence obtain better performance.

5.3 Zero-shot Generalization Performance (RQ2)

In this section, we conduct the zero-shot generalization to 20D F1~F16 synthetic problems, expensive problems and realistic problems to answer RQ2. Specifically, we use the RLDE-AFL model trained with 10D synthetic training set $\mathcal{I}_{\text{train}}$ to the aforementioned testing problem sets without further tuning. The RL-based baselines are also zero-shot generalized in the same way as RLDE-AFL.

5.3.1 Zero-shot to 20D problems. This section generalizes baselines from 10D training problem instances to 20D instances. As presented in Table 2, RLDE-AFL maintains the advantages and surpasses the baselines, showing the promising generalization across problem dimensions. The cross-dimension attention in NeurELA based feature extractor enables the agent to process populations with different dimensions uniformly and successfully capture the optimization information, while some baselines such as RL-DAS fails in generalization due to its dimension-dependent state design.

5.3.2 Zero-shot to expensive problems. In this section we reduce the maximum function evaluations from 20,000 to 2,000 and hence shorten the optimization horizon to simulate the expensive optimization scenarios in which maximum function evaluations are more limited. The problem instances in these scenarios would be much more challenging. We compare RLDE-AFL and 4 best baselines in 10D comparison: MadDE, NL-SHADE-LBC, DE-DDQN and

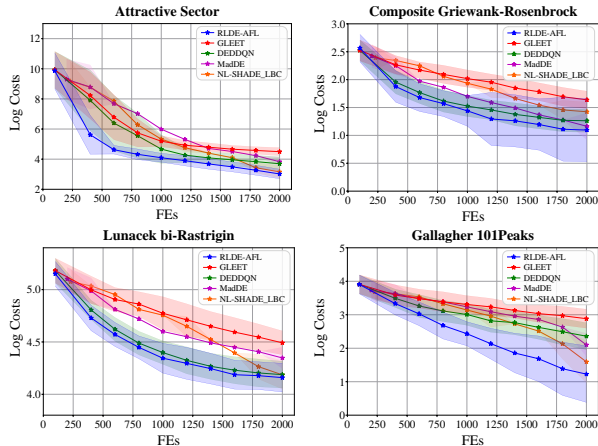


Figure 3: The optimization curves of RLDE-AFL and baselines on the four problems with 2,000 function evaluations.

GLEET. Figure 3 presents the optimization curves of the baselines under 4 10D synthetic problem instances in MetaBox: Attractive Sector (F2), Composite Griewank-Rosenbrock (F12), Lunacek bi-Rastrigin (F16) and Gallagher 101Peaks (training problem). The results show that RLDE-AFL has faster convergence speed in expensive scenarios and hence surpasses the 4 baselines. The results infer the potential of applying the RLDE-AFL models pre-trained on non-expensive problem instances to solve expensive problems, saving training cost while obtaining promising performance.

5.3.3 Zero-shot to realistic problems. The experiments above are conducted on synthetic problems which are in the same distribution as synthetic training problem instances. To further validate the generalization ability of RLDE-AFL on out-of-distribution problems, we employ the Protein-Docking problems [19] provided in MetaBox benchmark which containing 280 12D protein-docking task instances. Due to the computationally expensive evaluations, the maximum number of function evaluations is set to 500. The default search range for the optimization is $[-5, 5]$. We zero-shot RLDE-AFL and RL-based baselines DE-DDQN and GLEET trained on 10D synthetic problem instances to the protein-docking benchmark. The best objective value AEI [33, 35] results between RLDE-AFL and the 4 best baselines MadDE, NL-SHADE-LBC, DE-DDQN and GLEET are presented in Figure 4, the details of the AEI metric is provided in Appendix C. On protein-docking problem instances, RLDE-AFL shows competitive performance with GLEET and surpasses DE-DDQN, MadDE and NL-SHADE-LBC, revealing the remarkable out-of-distribution generalization ability of RLDE-AFL.

5.4 Ablation Study (RQ3)

In order to verify the effectiveness of the neural network based feature extractor, we conduct the ablation studies on the state design and feature extractor. We first remove the time stamp feature in the state and use NeurELA features only (denoted as “w/o Time”). Then we further ablate the mantissa-exponent representation and apply the min-max normalization adopted in original NeurELA (denoted



Figure 4: The AEI scores of RLDE-AFL and the baselines on the protein-docking realistic problem set.

Table 3: The averaged accumulated rewards of the ablated baselines and RLDE-AFL.

	w/o Time	w/o ME	MLP	HandCraft	RLDE-AFL
10D problems	9.497e-1 ±1.231e-2	9.442e-1 ±1.135e-2	9.451e-1 ±1.419e-2	9.512e-1 ±9.478e-3	9.645e-1 ±6.577e-3
20D problems	9.289e-01 ±1.500e-02	9.207e-01 ±1.592e-02	9.274e-01 ±1.414e-02	9.317e-01 ±1.243e-02	9.334e-01 ±1.295e-02
Expensive problems	8.836e-01 ±3.069e-02	8.713e-01 ±2.950e-02	8.847e-01 ±3.079e-02	8.714e-01 ±2.767e-02	8.856e-01 ±2.494e-02
Realistic problems	6.279e-01 ±1.475e-03	5.664e-01 ±1.300e-03	6.603e-01 ±1.535e-03	6.565e-01 ±1.519e-03	7.056e-01 ±1.608e-03

as “w/o ME”) for evaluation value normalization. Next we replace the attention modules in NeurELA by simple MLPs to validate the necessity of the information sharing between solutions and dimensions (denoted as “MLP”). Lastly we remove the whole NeurELA and instead use human-crafted optimization features proposed in GLEET as the states (denoted as “HandCraft”). The boxplots of the accumulated rewards of RLDE-AFL and the ablated baselines on 10D, 20D, expensive and realistic testing problems are presented in Table 3. The RLDE-AFL variant without time stamp feature slightly underperforms RLDE-AFL. The RL agent informed with optimization progress information could accordingly adjust the configuration along the optimization and hence achieve better performance. The baseline “w/o ME” uses min-max normalization within the populations which fails in distinguishing different instances and different optimization progresses, leading to poor performance. It confirms the necessity of the mantissa-exponent representation which not only normalizes the scales but also provides the agent exact performance of the individuals thereby supporting purposeful configuration. The lower performance of the MLP baseline validates the significance of the information sharing between individuals and dimensions in comprehensive decision-making. The superior performance of RLDE-AFL over the baseline with hand-crafted features emphasizes the effectiveness of the neural network based feature extractor, which relieves the human effort burden while acquiring better performance.

6 Conclusion

This paper proposed a novel MetaBBO approach, RLDE-AFL, with RL-based policy, generalizable NeurELA based feature extractor and diverse mutation and crossover operators. By integrating the attention-based learnable feature extraction module with mantissa-exponent based fitness representation to encode the population

and evaluation values into expressive optimization states, we relieved the expertise dependency in feature design and enhanced the generalization ability. We formulated the optimization process as a MDP and incorporated a comprehensive algorithm configuration space including the integrated diverse DE operators into a RL-aided algorithm configuration paradigm. Experimental results verified that the proposed RLDE-AFL not only showed promising optimization performance on in-distribution synthetic problems, but also presented robust generalization ability across problem dimensions and optimization horizons, as well as the out-of-distribution realistic BBO scenarios. In-depth analysis on state feature extraction further validated the effectiveness of the NeurELA module and the necessity of co-training the proposed feature learning module.

Acknowledgments

This work was supported in part by the National Natural Science Foundation of China No. 62276100, in part by the Guangdong Provincial Natural Science Foundation for Outstanding Youth Team Project No. 2024B1515040010, in part by the Guangdong Natural Science Funds for Distinguished Young Scholars No. 2022B1515020049, and in part by the TCL Young Scholars Program.

References

- [1] Jimmy Lei Ba, Jamie Ryan Kiros, and Geoffrey E Hinton. 2016. Layer normalization. In *NeurIPS*.
- [2] Subhodip Biswas, Debanjan Saha, Shuvodeep De, Adam D Cobb, Swagatam Das, and Brian A Jalaian. 2021. Improving differential evolution through Bayesian hyperparameter optimization. In *2021 IEEE Congress on Evolutionary Computation (CEC)*. 832–840.
- [3] Subhodip Biswas, Debanjan Saha, Shuvodeep De, Adam D Cobb, Swagatam Das, and Brian A Jalaian. 2021. Improving differential evolution through Bayesian hyperparameter optimization. In *CEC*. 832–840.
- [4] Janez Brest, Sao Greiner, Borko Boskovic, Marjan Mernik, and Viljem Zumer. 2006. Self-adapting control parameters in differential evolution: A comparative study on numerical benchmark problems. *IEEE Transactions on Evolutionary Computation* 10, 6 (2006), 646–657.
- [5] Janez Brest, Mirjam Sepesy Maučec, and Borko Bošković. 2021. Self-adaptive differential evolution algorithm with population size reduction for single objective bound-constrained optimization: Algorithm j21. In *2021 IEEE Congress on Evolutionary Computation (CEC)*. 817–824.
- [6] Janez Brest, Mirjam Sepesy Maučec, and Borko Bošković. 2021. Self-adaptive differential evolution algorithm with population size reduction for single objective bound-constrained optimization: Algorithm j21. In *CEC*. 817–824.
- [7] Jiacheng Chen, Zeyuan Ma, Hongshu Guo, Yining Ma, Jie Zhang, and Yue-Jiao Gong. 2024. SYMBOL: Generating Flexible Black-Box Optimizers through Symbolic Equation Learning. In *ICLR*.
- [8] Michael G Epitropakis, Dimitris K Tasoulis, Nicos G Pavlidis, Vassilis P Plagianakos, and Michael N Vrahatis. 2011. Enhancing differential evolution utilizing proximity-based mutation operators. *IEEE Transactions on Evolutionary Computation* 15, 1 (2011), 99–119.
- [9] Iztok Fister, Dušan Fister, and Iztok Fister Jr. 2022. Reinforcement learning-based differential evolution for global optimization. In *Differential Evolution: From Theory to Practice*. 43–75.
- [10] Hongshu Guo, Yining Ma, Zeyuan Ma, Jiacheng Chen, Xinglin Zhang, Zhiguang Cao, Jun Zhang, and Yue-Jiao Gong. 2024. Deep Reinforcement Learning for Dynamic Algorithm Selection: A Proof-of-Principle Study on Differential Evolution. *TSMC* (2024).
- [11] Yupeng Han, Hu Peng, Changrong Mei, Lianglin Cao, Changshou Deng, Hui Wang, and Zhijian Wu. 2023. Multi-strategy multi-objective differential evolutionary algorithm with reinforcement learning. *KBS* 277 (2023), 110801.
- [12] Nikolaus Hansen, Steffen Finck, Raymond Ros, and Anne Auger. 2009. *Real-parameter black-box optimization benchmarking 2009: Noiseless functions definitions*. Ph.D. Dissertation. INRIA.
- [13] John H Holland. 1992. *Adaptation in natural and artificial systems: an introductory analysis with applications to biology, control, and artificial intelligence*. MIT press.
- [14] Zhenzhen Hu and Wenyin Gong. 2022. Constrained evolutionary optimization based on reinforcement learning using the objective function and constraints. *KBS* 237 (2022), 107731.
- [15] Zhenzhen Hu, Wenyin Gong, and Shuijia Li. 2021. Reinforcement learning-based differential evolution for parameters extraction of photovoltaic models. *Energy Rep.* 7 (2021), 916–928.
- [16] Zhenzhen Hu, Wenyin Gong, Witold Pedrycz, and Yanchi Li. 2023. Deep reinforcement learning assisted co-evolutionary differential evolution for constrained optimization. *Swarm Evol. Comput.* 83 (2023), 101387.
- [17] Ying Huang, Wei Li, Furong Tian, and Xiang Meng. 2020. A fitness landscape ruggedness multiobjective differential evolution algorithm with a reinforcement learning strategy. *Appl. Soft Comput.* 96 (2020), 106693.
- [18] Thanh N Huynh, Dieu TT Do, and Jaehong Lee. 2021. Q-Learning-based parameter control in differential evolution for structural optimization. *Appl. Soft Comput.* 107 (2021), 107464.
- [19] Howook Hwang, Thom Vreven, Joël Janin, and Zhiping Weng. 2010. Protein-protein docking benchmark version 4.0. *Proteins: Structure, Function, and Bioinformatics* 78, 15 (2010), 3111–3114.
- [20] Sk Minhazul Islam, Swagatam Das, Saurav Ghosh, Subhrajit Roy, and Ponnuthurai Nagarathnam Suganthan. 2011. An adaptive differential evolution algorithm with novel mutation and crossover strategies for global numerical optimization. *TSMC* 42, 2 (2011), 482–500.
- [21] James Kennedy and Russell Eberhart. 1995. Particle swarm optimization. In *ICNN*, Vol. 4. IEEE, 1942–1948.
- [22] Abhishek Kumar, K. V. Price, Ali Wagdy Mohamed, Anas A Hadi, and P. N. Suganthan. 2022. Problem definitions and evaluation criteria for the CEC 2022 special session and competition on single objective bound constrained numerical optimization. In *Tech. Rep.* Singapore: Nanyang Technological University.
- [23] Xiaobin Li, Kai Wu, Yujian Betterest Li, Xiaoyu Zhang, Handing Wang, and Jing Liu. 2024. GLHF: General Learned Evolutionary Algorithm Via Hyper Functions. *arXiv preprint arXiv:2405.03728* (2024).
- [24] Xiaobin Li, Kai Wu, Yujian Betterest Li, Xiaoyu Zhang, Handing Wang, and Jing Liu. 2024. Pretrained Optimization Model for Zero-Shot Black Box Optimization. In *The Thirty-eighth Annual Conference on Neural Information Processing Systems*. <https://openreview.net/forum?id=fWQhXdeuSG>
- [25] Xiaobin Li, Kai Wu, Xiaoyu Zhang, and Handing Wang. 2024. B2Opt: Learning to Optimize Black-box Optimization with Little Budget. In *The 39th Annual AAAI Conference on Artificial Intelligence*. <https://openreview.net/forum?id=i2KEFyC4dq>
- [26] Yuzhen Li, Shihao Wang, Hongyu Yang, Hu Chen, and Bo Yang. 2023. Enhancing differential evolution algorithm using leader-adjoint populations. *Information Sciences* 622 (2023), 235–268.
- [27] Zhihui Li, Li Shi, Caitong Yue, Zhigang Shang, and Boyang Qu. 2019. Differential evolution based on reinforcement learning with fitness ranking for solving multimodal multiobjective problems. *Swarm Evol. Comput.* 49 (2019), 234–244.
- [28] Hongqiao Lian, Zeyuan Ma, Hongshu Guo, Ting Huang, and Yue-Jiao Gong. 2024. Rlemmo: Evolutionary multimodal optimization assisted by deep reinforcement learning. In *GECCO*. 683–693.
- [29] Zuowen Liao, Qishuo Pang, and Qiong Gu. 2024. Differential evolution based on strategy adaptation and deep reinforcement learning for multimodal optimization problems. *Swarm Evol. Comput.* 87 (2024), 101568.
- [30] Xin Liu, Jianyong Sun, Qingfu Zhang, Zhenkun Wang, and Zongben Xu. 2023. Learning to learn evolutionary algorithm: A learnable differential evolution. *TETCI* 7, 6 (2023), 1605–1620.
- [31] Zeyuan Ma, Jiacheng Chen, Hongshu Guo, and Yue-Jiao Gong. 2024. Neural exploratory landscape analysis. *arXiv preprint arXiv:2408.10672* (2024).
- [32] Zeyuan Ma, Jiacheng Chen, Hongshu Guo, Yining Ma, and Yue-Jiao Gong. 2024. Auto-configuring Exploration-Exploitation Tradeoff in Evolutionary Computation via Deep Reinforcement Learning. In *GECCO*. 1497–1505.
- [33] Zeyuan Ma, Hongshu Guo, Jiacheng Chen, Zhenrui Li, Guojun Peng, Yue-Jiao Gong, Yining Ma, and Zhiguang Cao. 2023. MetaBox: A Benchmark Platform for Meta-Black-Box Optimization with Reinforcement Learning. In *NeurIPS*, Vol. 36.
- [34] Zeyuan Ma, Hongshu Guo, Jiacheng Chen, Guojun Peng, Zhiguang Cao, Yining Ma, and Yue-Jiao Gong. 2024. LLaMoCo: Instruction Tuning of Large Language Models for Optimization Code Generation. *arXiv preprint arXiv:2403.01131* (2024).
- [35] Zeyuan Ma, Hongshu Guo, Yue-Jiao Gong, Jun Zhang, and Kay Chen Tan. 2024. Toward Automated Algorithm Design: A Survey and Practical Guide to Meta-Black-Box-Optimization. *arXiv preprint arXiv:2411.00625* (2024).
- [36] Zhenyu Meng and Jeng-Shyang Pan. 2019. HARD-DE: Hierarchical archive based mutation strategy with depth information of evolution for the enhancement of differential evolution on numerical optimization. *IEEE Access* 7 (2019), 12832–12854.
- [37] Volodymyr Mnih. 2013. Playing atari with deep reinforcement learning. *arXiv preprint* (2013).
- [38] Ali Wagdy Mohamed, Anas A Hadi, Ali Khater Mohamed, Prachi Agrawal, Abhishek Kumar, and P. N. Suganthan. 2021. *Problem definitions and evaluation criteria for the CEC 2021 Special Session and Competition on Single Objective Bound Constrained Numerical Optimization*. Technical Report.
- [39] Jiuyan Pei, Jialin Liu, and Yi Mei. 2024. Learning from Offline and Online Experiences: A Hybrid Adaptive Operator Selection Framework. In *GECCO*.

- 1017–1025.
- [40] Lei Peng, Zhuoming Yuan, Guangming Dai, Maocai Wang, and Zhe Tang. 2023. Reinforcement learning-based hybrid differential evolution for global optimization of interplanetary trajectory design. *Swarm Evol. Comput.* 81 (2023), 101351.
- [41] Raphael Patrick Prager, Moritz Vinzent Seiler, Heike Trautmann, and Pascal Kerschke. 2021. Towards feature-free automated algorithm selection for single-objective continuous black-box optimization. In *2021 IEEE Symposium Series on Computational Intelligence (SSCI)*. IEEE, 1–8.
- [42] Kangjia Qiao, Xupeng Wen, Xuanxuan Ban, Peng Chen, Kenneth V. Price, Ponnuthurai N. Suganthan, Jing Liang, Guohua Wu, and Caitong Yue. 2024. *Evaluation criteria for CEC 2024 competition and special session on numerical optimization considering accuracy and speed*. Technical Report.
- [43] A Kai Qin and Ponnuthurai N Suganthan. 2005. Self-adaptive differential evolution algorithm for numerical optimization. In *2005 IEEE Congress on Evolutionary Computation*, Vol. 2. IEEE, 1785–1791.
- [44] Wagner F Sacco and Nélio Henderson. 2014. Differential evolution with topographical mutation applied to nuclear reactor core design. *Progress in Nuclear Energy* 70 (2014), 140–148.
- [45] Karam M Sallam, Saber M Elsayed, Ripon K Chakraborty, and Michael J Ryan. 2020. Evolutionary framework with reinforcement learning-based mutation adaptation. *IEEE Access* 8 (2020), 194045–194071.
- [46] John Schulman, Filip Wolski, Prafulla Dhariwal, Alec Radford, and Oleg Klimov. 2017. Proximal policy optimization algorithms. *arXiv preprint arXiv:1707.06347* (2017).
- [47] Moritz Vinzent Seiler, Pascal Kerschke, and Heike Trautmann. 2025. Deep-ela: Deep exploratory landscape analysis with self-supervised pretrained transformers for single-and multi-objective continuous optimization problems. *Evolutionary Computation* (2025), 1–27.
- [48] Mudita Sharma, Alexandros Komninos, Manuel López-Ibáñez, and Dimitar Kazakov. 2019. Deep reinforcement learning based parameter control in differential evolution. In *GECCO*. 709–717.
- [49] Vladimir Stanovov, Shakhnaz Akhmedova, and Eugene Semenkin. 2022. NL-SHADE-LBC algorithm with linear parameter adaptation bias change for CEC 2022 Numerical Optimization. In *2022 IEEE Congress on Evolutionary Computation (CEC)*. IEEE, 01–08.
- [50] Vladimir Stanovov, Shakhnaz Akhmedova, and Eugene Semenkin. 2022. NL-SHADE-LBC algorithm with linear parameter adaptation bias change for CEC 2022 Numerical Optimization. In *CEC*. 01–08.
- [51] Vladimir Stanovov and Eugene Semenkin. 2024. Success Rate-based Adaptive Differential Evolution L-SRTDE for CEC 2024 Competition. In *2024 IEEE Congress on Evolutionary Computation (CEC)*. IEEE, 1–8.
- [52] Rainer Storn and Kenneth Price. 1997. Differential evolution—a simple and efficient heuristic for global optimization over continuous spaces. *J. Glob. Optim.* 11 (1997), 341–359.
- [53] Jianyong Sun, Xin Liu, Thomas Bäck, and Zongben Xu. 2021. Learning adaptive differential evolution algorithm from optimization experiences by policy gradient. *TEC* 25, 4 (2021), 666–680.
- [54] Zhiping Tan and Kangshun Li. 2021. Differential evolution with mixed mutation strategy based on deep reinforcement learning. *Appl. Soft Comput.* 111 (2021), 107678.
- [55] Zhiping Tan, Yu Tang, Kangshun Li, Huasheng Huang, and Shaoming Luo. 2022. Differential evolution with hybrid parameters and mutation strategies based on reinforcement learning. *Swarm Evol. Comput.* 75 (2022), 101194.
- [56] Zhiping Tan, Yu Tang, Kangshun Li, Huasheng Huang, and Shaoming Luo. 2022. Differential evolution with hybrid parameters and mutation strategies based on reinforcement learning. *Swarm Evol. Comput.* 75 (2022), 101194.
- [57] Ryoji Tanabe and Alex Fukunaga. 2013. Success-history based parameter adaptation for differential evolution. In *2013 IEEE Congress on Evolutionary Computation*. 71–78.
- [58] Hado Van Hasselt, Arthur Guez, and David Silver. 2016. Deep reinforcement learning with double q-learning. In *AAAI*.
- [59] Ashish Vaswani, Noam Shazeer, Niki Parmar, Jakob Uszkoreit, Llion Jones, Aidan N Gomez, Łukasz Kaiser, and Illia Polosukhin. 2017. Attention is all you need. *Advances in Neural Information Processing Systems* (2017).
- [60] Yong Wang, Zixing Cai, and Qingfu Zhang. 2011. Differential evolution with composite trial vector generation strategies and control parameters. *IEEE transactions on evolutionary computation* 15, 1 (2011), 55–66.
- [61] Christopher JCH Watkins and Peter Dayan. 1992. Q-learning. *Mach. Learn.* 8 (1992), 279–292.
- [62] David H Wolpert, William G Macready, et al. 1995. *No free lunch theorems for search*. Technical Report. Citeseer.
- [63] Sewall Wright et al. 1932. The roles of mutation, inbreeding, crossbreeding, and selection in evolution. (1932).
- [64] Kai Wu, Xiaobin Li, Penghui Liu, and Jing Liu. 2023. DECN: Evolution inspired deep convolution network for black-box optimization. *arXiv preprint arXiv:2304.09599* (2023).
- [65] Sheng-Hao Wu, Yuxiao Huang, Xingyu Wu, Liang Feng, Zhi-Hui Zhan, and Kay Chen Tan. 2024. Learning to Transfer for Evolutionary Multitasking. *arXiv preprint* (2024).
- [66] Hai Xia, Changhe Li, Sanyou Zeng, Qingshan Tan, Junchen Wang, and Shengxiang Yang. 2021. A reinforcement-learning-based evolutionary algorithm using solution space clustering for multimodal optimization problems. In *CEC*. 1938–1945.
- [67] Qingyong Yang, Shu-Chuan Chu, Jeng-Shyang Pan, Jyh-Horng Chou, and Junzo Watada. 2023. Dynamic multi-strategy integrated differential evolution algorithm based on reinforcement learning for optimization problems. *Complex Intell. Syst.* (2023), 1–33.
- [68] Xu Yang, Rui Wang, and Kaiwen Li. 2024. Meta-Black-Box Optimization for Evolutionary Algorithms: Review and Perspective. *Available at SSRN 4956956* (2024).
- [69] Chenxi Ye, Chengjun Li, Yang Li, Yufei Sun, Wenxuan Yang, Mingyuan Bai, Xuanyu Zhu, Jinghan Hu, Tingzi Chi, Hongbo Zhu, et al. 2023. Differential evolution with alternation between steady monopoly and transient competition of mutation strategies. *Swarm and Evolutionary Computation* 83 (2023), 101403.
- [70] Xiaobing Yu, Pingping Xu, Feng Wang, and Xuming Wang. 2024. Reinforcement learning-based differential evolution algorithm for constrained multi-objective optimization problems. *EAAI* 131 (2024), 107817.
- [71] Haotian Zhang, Jialong Shi, Jianyong Sun, Ali Wagdy Mohamed, and Zongben Xu. 2024. A Gradient-based Method for Differential Evolution Parameter Control by Smoothing. In *GECCO*. 423–426.
- [72] Haotian Zhang, Jianyong Sun, Thomas Bäck, and Zongben Xu. 2024. Learning to select the recombination operator for derivative-free optimization. *Sci. China Math.* (2024), 1–24.
- [73] Haotian Zhang, Jianyong Sun, Thomas Bäck, Qingfu Zhang, and Zongben Xu. 2023. Controlling Sequential Hybrid Evolutionary Algorithm by Q-Learning [Research Frontier] [Research Frontier]. *CIM* 18, 1 (2023), 84–103.
- [74] Jingqiao Zhang and Arthur C Sanderson. 2009. JADE: adaptive differential evolution with optional external archive. *IEEE Transactions on Evolutionary Computation* 13, 5 (2009), 945–958.
- [75] Qi Zhao, Tengfei Liu, Bai Yan, Qiqi Duan, Jian Yang, and Yuhui Shi. 2024. Automated Metaheuristic Algorithm Design with Autoregressive Learning. *arXiv preprint* (2024).

A Operator Collection

In this section we list the names, formulations, descriptions and configuration spaces of the integrated DE mutation and crossover operators in Table 4.

Table 4: The names, formulations, descriptions and configuration spaces of the integrated DE mutation and crossover operators.

Index	Operator	Formula	Description	Parameter
1	rand/1	$u = x_{r1} + F \cdot (x_{r2} - x_{r3})$	Generate exploratory trail solutions using 3 randomly selected individuals x_r .	$F \in [0, 1]$
2	best/1	$u = x^* + F \cdot (x_{r1} - x_{r2})$	Generate exploitative trail solutions by leveraging the best individual x^* from the current population and random individuals.	$F \in [0, 1]$
3	rand/2	$u = x_{r1} + F \cdot (x_{r2} - x_{r3}) + F \cdot (x_{r4} - x_{r5})$	Generate exploratory trail solution with 5 randomly selected individuals, enhancing the exploration of rand/1.	$F \in [0, 1]$
4	best/2	$u = x^* + F \cdot (x_{r1} - x_{r2}) + F \cdot (x_{r3} - x_{r4})$	Generate exploitative trail solutions by leveraging the best individual and 4 random individuals, which is more exploratory than best/1.	$F \in [0, 1]$
5	current-to-rand/1	$u = x + F \cdot (x_{r1} - x) + F \cdot (x_{r2} - x_{r3})$	Generate trail solution by leveraging the current individual x and random individuals.	$F \in [0, 1]$
6	current-to-best/1	$u = x + F \cdot (x^* - x) + F \cdot (x_{r1} - x_{r2})$	Generate trail solution by leveraging the current individual x and the best solution x^* .	$F \in [0, 1]$
7	rand-to-best/1	$u = x_{r1} + F \cdot (x^* - x_{r2}) + F \cdot (x_{r3} - x_{r4})$	Generate trail solution by leveraging the random individuals x_r and the best solution x^* from the current population.	$F \in [0, 1]$
8	current-to-pbest/1 [20]	$u = x + F \cdot (x_p^* - x) + F \cdot (x_{r1} - x_{r2})$	A variant of current-to-best/1, replace the best individual with the individual randomly selected from the top $p\%$ individuals in the population x_p^* for better exploration.	$F \in [0, 1]$ $p \in [0, 1]$
9	current-to-pbest/1 + archive [74]	$u = x + F \cdot (x_p^* - x) + F \cdot (x_{r1} - \tilde{x}_{r2})$	A variant of current-to-pbest/1, replace the last random individual with a individual randomly selected from the union of the population and archive \tilde{x}_r , to further enhance the exploration.	$F \in [0, 1]$ $p \in [0, 1]$
10	current-to-rand/1 + archive [3]	$u = x + F \cdot (x_{r1} - \tilde{x}_{r2})$	A variant of current-to-rand/1, which also replaces the last random individual with a individual randomly selected from the union of the population and archive \tilde{x}_r .	$F \in [0, 1]$
11	weighted-rand-to-pbest/1 [3]	$u = F \cdot x_{r1} + F \cdot F_a \cdot (x_p^* - x_{r2})$	A variant of rand-to-best/1, replace the best individual with the individual randomly selected from the top $p\%$ individuals in the population x_p^* , and add a new parameter to enhance the behaviour diversity.	$F \in [0, 1]$ $F_a \in [0, 1]$ $p \in [0, 1]$
12	ProDE-rand/1 [8]	$u = x_{p1} + F \cdot (x_{p2} - x_{p3})$	A variant of rand/1, which takes the distances between individuals into consideration and assigns close individuals larger selection probabilities, enhancing the exploitation of rand/1.	$F \in [0, 1]$
13	HARDDE-current-to-pbest/2 [36]	$u = x + F \cdot (x_p^* - x) + F_1 \cdot (x_{r1} - \tilde{x}_{r2}) + F_1 \cdot (x_{r1} - \tilde{x}_{r3})$	A variant of current-to-pbest/1, replace the last random individual with a individual randomly selected from the union of the population and archive \tilde{x}_{r2} , and add a solution difference using the individual \tilde{x}_{r3} randomly selected from the union of the population and former individual archive.	$F \in [0, 1]$ $F_1 \in [0, 1]$ $p \in [0, 1]$
14	TopoDE-rand/1 [44]	$u = x_{nb} + F \cdot (x_{r2} - x_{r3})$	A variant of rand/1, use the best individual x_{nb} in the nearest individuals to replace the first random individual in rand/1.	$F \in [0, 1]$
1	binomial crossover	$v_j = \begin{cases} u_j & \text{If } rand_j < Cr \text{ or } j = jrand; \\ x_j & \text{Otherwise.} \end{cases} \quad j = 1, 2, \dots, D$	Basic crossover operator that randomly selects values from trail solution or parent solution and uses a random index $jrand$ to ensure that the generated individual is different from the parent.	$Cr \in [0, 1]$
2	exponential crossover	$v_j = \begin{cases} u_j & \text{If } j \in \{(n)_D, (n+1)_D, \dots, (n+L-1)_D\}; \\ x_j & \text{Otherwise.} \end{cases} \quad j = 1, 2, \dots, D$	Basic crossover operator that randomly selects a random length segment of the parent and cover the parent values in this segment using trail solution values.	$Cr \in [0, 1]$
3	p-binomial crossover [3]	$v_j = \begin{cases} u_j & \text{If } rand_j < Cr \text{ or } j = jrand; \\ x_j^p & \text{Otherwise.} \end{cases} \quad j = 1, 2, \dots, D$	A variant of binomial crossover which replaces the parent individual with the individual randomly selected from the top $p\%$ individuals in the population x_p^* .	$Cr \in [0, 1]$ $p \in [0, 1]$

B Training & Testing Problem Set

MetaBox provides 24 synthetic problem instances with diverse characteristics and landscapes as listed in Table 5. Figure 5 and Figure 6 presents the landscapes of the training and testing problem instances when dimensions are set to 2, respectively. We select $f_1, f_2, f_3, f_5, f_{15}, f_{16}, f_{17}$ and f_{21} as training functions and the rest for testing to balance the optimization difficulty in training and testing problem sets.

Table 5: Overview of the BBOB testsuites.

	Problem	Functions
Separable functions	f_1	Sphere Function
	f_2	Ellipsoidal Function
	f_3	Rastrigin Function
	f_4	Buche-Rastrigin Function
	f_5	Linear Slope
Functions with low or moderate conditioning	f_6	Attractive Sector Function
	f_7	Step Ellipsoidal Function
	f_8	Rosenbrock Function, original
	f_9	Rosenbrock Function, rotated
Functions with high conditioning and unimodal	f_{10}	Ellipsoidal Function
	f_{11}	Discus Function
	f_{12}	Bent Cigar Function
	f_{13}	Sharp Ridge Function
	f_{14}	Different Powers Function
Multi-modal functions with adequate global structure	f_{15}	Rastrigin Function (non-separable counterpart of F3)
	f_{16}	Weierstrass Function
	f_{17}	Schaffers F7 Function
	f_{18}	Schaffers F7 Function, moderately ill-conditioned
	f_{19}	Composite Griewank-Rosenbrock Function F8F2
Multi-modal functions with weak global structure	f_{20}	Schwefel Function
	f_{21}	Gallagher's Gaussian 101-me Peaks Function
	f_{22}	Gallagher's Gaussian 21-hi Peaks Function
	f_{23}	Katsuura Function
	f_{24}	Lunacek bi-Rastrigin Function
		Default search range: $[-5, 5]^D$

C AEI Metric

In Section 5.3.3 in the main paper, we present the best objective value AEI scores of the baselines for validating the zero-shot performance on realistic problems. To get the score, we test the target approach on K problem instances for G repeated runs and then record the basic

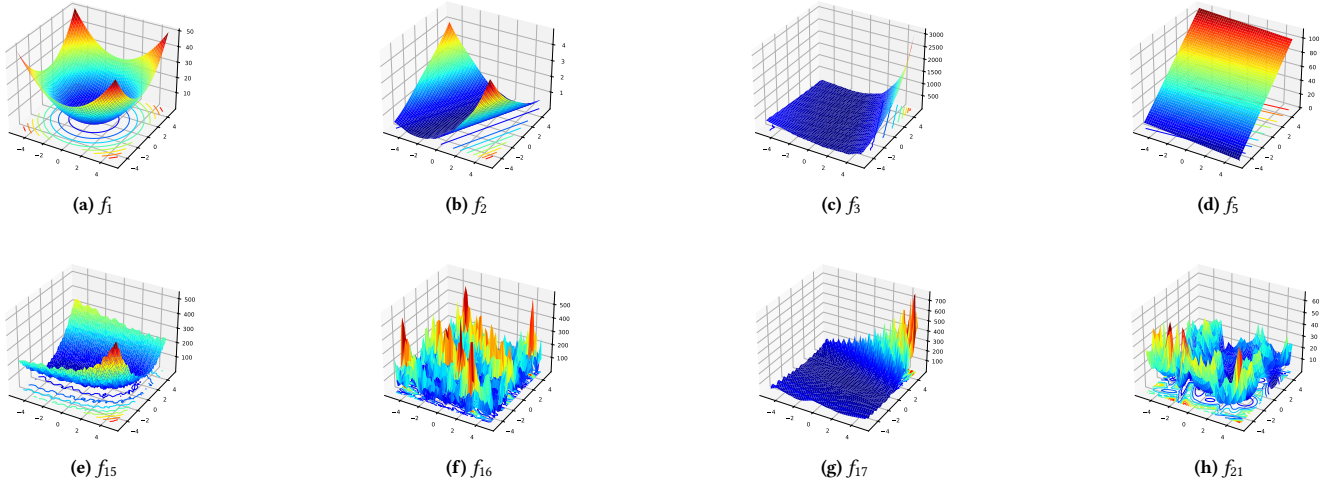


Figure 5: Fitness landscapes of functions in the training set when dimension is set to 2.

metrics. The best objective value $v_{obj}^{k,g}$ denotes the best objective found by the algorithm on the k -th problem during the g -th test run. To convert its monotonicity, we conduct an inverse transformation, i.e., $v_{obj}^{k,g} = \frac{1}{v_{obj}^{k,g}}$. Then, Z-score normalization is applied:

$$Z^k = \frac{1}{G} \sum_{g=1}^G \frac{v_{obj}^{k,g} - \mu_*}{\sigma_*}, \quad (8)$$

where μ_* and σ_* are calculated by using Random Search as a baseline. Finally, the best objective value AEI score is calculated by:

$$AEI = \frac{1}{K} \sum_{k=1}^K e^{Z^k}, \quad (9)$$

where Z-scores are first aggregated, then subjected to an inverse logarithmic transformation, and subsequently averaged across the test problem instances. A higher AEI indicates better performance of the corresponding approach.

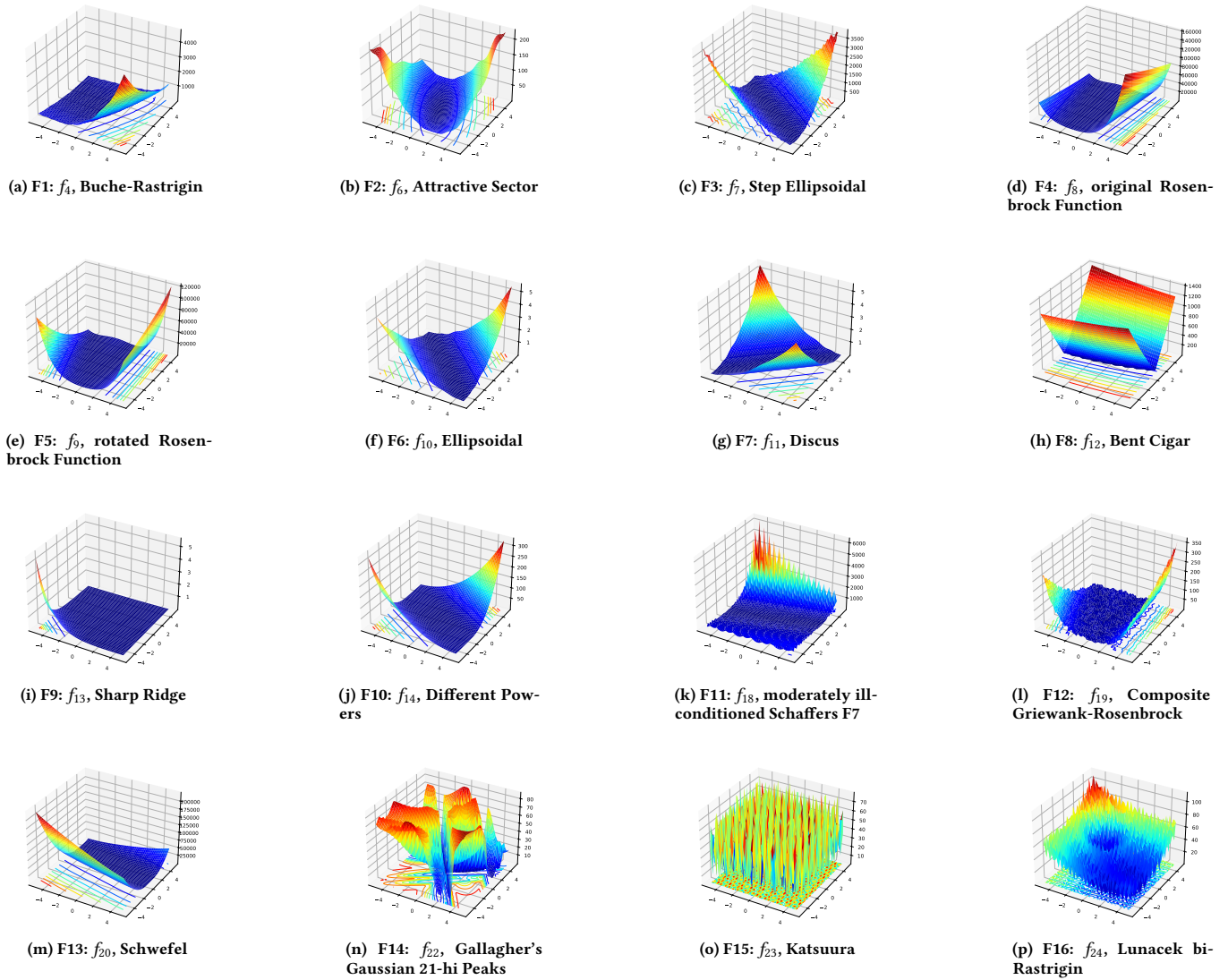


Figure 6: Fitness landscapes of functions in the testing set when dimension is set to 2.